An Observational Study of Environmental Dynamical Control of Tropical Cyclone Intensity in the Atlantic

ZHIHUA ZENG

Nanjing University of Information Science and Technology, Nanjing, and Shanghai Typhoon Institute, China Meteorological Administration, Shanghai, China

LIANSHOU CHEN

Chinese Academy of Meteorological Sciences, China Meteorological Administration, Beijing, China

YUQING WANG

International Pacific Research Center, and Department of Meteorology, School of Ocean and Earth Science and Technology, University of Hawaii at Manoa, Honolulu, Hawaii

(Manuscript received 20 September 2007, in final form 6 February 2008)

ABSTRACT

An attempt has been made to extend the analysis of environmental dynamical control of tropical cyclone (TC) intensity recently performed for the western North Pacific to the North Atlantic. The results show that both the vertical shear and translational speed have negative effects on TC intensity, which is consistent with previous findings for other basins. It shows that few TCs intensified when they moved faster than 15 m s^{-1}. The threshold vertical shear of 20 m s^{-1}—defined as the difference of total winds between 200 and 850 hPa averaged within 5° latitude around the TC center—is found above which few TCs intensified and below which most TCs could reach their lifetime peak intensity. The average intensity of total TCs in the Atlantic is a bit smaller than that in the western North Pacific. The SST-determined empirical maximum potential intensity (EMPI) for a TC for 1981–2003 in this study is slightly higher than that found for 1962–92 by DeMaria and Kaplan in the Atlantic, however.

To be consistent with the theoretical TC MPI, a new EMPI has been constructed, which includes the effect of thermodynamic efficiency. This new EMPI marginally improves the estimation of real TC maximum intensity because the thermodynamic efficiency is largely determined by SST. To include the environmental dynamical control of TC intensity, a dynamical efficiency has been introduced, which is inversely proportional to the combined amplitude of the vertical shear and translational speed. With this dynamical efficiency, an empirical maximum intensity (EMI) for Atlantic TCs has been constructed. This EMI includes not only the positive contribution by SST but also the effects of both thermodynamic and dynamical efficiencies, and it provides more accurate estimations of TC maximum intensity. Furthermore, the formulation of the new EMI explains the observed behavior of TC maximum intensity by thermodynamic and dynamical controls in a transparent and easy-to-interpret manner.

1. Introduction

In a recent study, Zeng et al. (2007, hereafter ZWW) performed an observational study on the environmental dynamical control of tropical cyclone (TC) intensity over the western North Pacific. Based on statistical analysis, they show that both the translational speed and vertical shear of horizontal wind in the large-scale environment can have marked effects on TC intensification rate, intensity, and lifetime peak intensity. They found that in general, the fast translation and strong vertical shear are negative to the TC intensification rate and lifetime peak intensity. In addition, the very intense TCs and the TCs with rapid intensification only occur in a narrow range of translational speed (between 3 and 8 m s^{-1}) and in relatively weak vertical shear. ZWW also show that few TCs intensified when they moved faster

Corresponding author address: Dr. Yuqing Wang, IPRC/SOEST, University of Hawaii at Manoa, 1680 East–West Road, POST Bldg., Room 409G, Honolulu, HI 96822.
E-mail: yuqing@hawaii.edu

DOI: 10.1175/2008MWR2388.1

than 15 m s^{-1} or when their large-scale environmental vertical shear is larger than 20 m s^{-1}.

With statistical analysis, ZWW also developed a new empirical maximum potential intensity (EMPI) for the western North Pacific. The new empirical MPI differs from earlier empirical MPI in that it includes the combined negative effect of the translational speed and vertical shear as the environmental dynamical control, in addition to the positive contribution of sea surface temperature (SST) and the outflow layer temperature as the thermodynamic control. They demonstrated that their new empirical MPI not only provides more accurate estimation of TC maximum intensity but also better explains the observed behavior of the TC maximum intensity and helps explain the thermodynamic and environmental dynamical controls of TC intensity in a transparent way.

Because the analysis of ZWW was based on observations for the western North Pacific TCs, a natural question arises as to whether the findings can be applied to other ocean basins, such as the North Atlantic basin. An effort is made in this study to extend a similar analysis to Atlantic TCs based on the best-track TC data, Reynolds SST, and the National Centers for Environmental Prediction–National Center for Atmospheric Research (NCEP–NCAR) reanalysis during 1981–2003. This period was chosen to be consistent with that used in ZWW for the western North Pacific. Thus, it facilitates a direct comparison between the two basins.

There have been several observational studies on the maximum intensity for the Atlantic TCs, but they are mainly based on the relationship between the TC MPI and SST. Merrill (1988) derived an empirical maximum TC intensity for a given SST by comparing climatological SSTs with the maximum sustained winds of Atlantic hurricanes. After removing the translational speed from the maximum sustained winds of Atlantic TCs that occurred between 1962 and 1992, DeMaria and Kaplan (1994a) developed an empirical MPI as a function of SST and used the climatological SSTs. DeMaria and Kaplan (1994a) also showed that most TCs could only reach 55% of their SST-determined MPIs and that only about 20% reach 80% or more of their MPIs at the time when they are most intense. One of the caveats of their empirical MPI is the lack of any dynamical control, such as environmental flow and vertical shear. Furthermore, they have not included the effect of outflow layer temperature, which is demonstrated to be important to the thermodynamic efficiency of a TC heat engine (Emanuel 1988, 1995).

The possible effect of vertical shear and translation on tropical cyclone structure and intensity has been studied numerically (e.g., Wang and Holland 1996; Bender 1997; Frank and Ritchie 1999, 2001), observationally (e.g., DeMaria and Kaplan 1994a; Elsberry and Jeffries 1996; Lonfat et al. 2004; Knaff et al. 2005; Chen et al. 2006), and theoretically (e.g., Shapiro 1983; Reasor et al. 2004). There is growing evidence that both the direction and the vertical profile of vertical shear is important (Wang and Holland 1996; Elsberry and Jeffries 1996; Bender 1997; Wang and Wu 2004). Vertical shear is more destructive to TCs at low latitudes and to small TCs (Jones 1995; DeMaria 1996). The variation of storm structure as functions of translational speed and vertical shear has been examined in some recent observational studies as well (e.g., Corbosiero and Molinari 2002, 2003; Lonfat et al. 2004; Chen et al. 2006).

The effects of translational speed and vertical shear on TC intensity are found to be statistically significant. Thus, they are included as predictors in the current operational statistical TC intensity prediction models for Atlantic TCs, such as the Statistical Hurricane Intensity Prediction Scheme (SHIPS; DeMaria and Kaplan 1994b, 1999; DeMaria et al. 2005). However, a detailed analysis for these predictors for Atlantic TCs is still lacking. This analysis would provide insights into understanding the importance of the environmental dynamical control of TC intensification and maximum intensity.

In this study, an analysis similar to that performed by ZWW for the western North Pacific is conducted, and the results are compared with those found in ZWW. Our objectives are as follows: 1) to examine the thermodynamic control of TC MPI over the Atlantic, including the thermodynamic efficiency; 2) to analyze the effects of translation and large-scale environmental vertical shear on TC intensification and intensity in the Atlantic; 3) to construct an empirical maximum intensity (EMI) for TCs in the region that includes not only the thermodynamic control of SST and outflow layer temperature but also the effects of storm translation and vertical shear of the environmental flow; and 4) to compare the results with those found for the western North Pacific TCs.

The rest of the paper is organized as follows: section 2 describes the data and methodology used in this study. The thermodynamic control of TC MPI is examined in section 3. Section 4 discusses the individual effects of translational speed and vertical shear and their combined effect on TC intensity, together with the construction of an EMI incorporating environmental dynamical control, namely, the effect of the dynamical efficiency. A summary and discussion are given in section 5.

2. Data and methodology

TC position and intensity, SST, and vertical shear of the large-scale environmental flow are the key parameters/fields examined in this study. The analysis is restricted to the period from 1981 to 2003 over the Atlantic Ocean, the same period that was used in the analysis for the western North Pacific in ZWW. This facilitates a comparison of the results in the two basins.

The TC position and intensity information was obtained from the National Hurricane Center–Tropical Prediction Center (NHC–TPC). The postanalyzed product data are the best determination of TC position and intensity, namely, "best track" (NHC–TPC), by considering additional information not used in the operational setting. The data contain 6-hourly TC latitude, longitude, and maximum sustained surface wind for all TCs designated by the NHC–TPC as being tropical storm strength with actual maximum sustained surface wind speeds greater than 17 m s^{-1}. Only TCs within the region of 0°–50°N, 20°–100°W were included in our analysis.

The SST data used are the Reynolds SST reanalysis provided by the National Oceanic and Atmospheric Administration–Cooperative Institute for Research in Environmental Sciences (NOAA–CIRES) Climate Diagnostics Center (CDC) and obtained from the CDC Web site (http://www.cdc.noaa.gov). The Reynolds SST is a weekly mean with a horizontal resolution of 1° latitude/longitude (Reynolds et al. 2002). The SST at a given time at the TC center is linearly interpolated in time from the weekly Reynolds SST, and it is interpolated in space using a bicubic spline interpolation.

NCEP–NCAR reanalysis products (Kalnay et al. 1996) were used to estimate the vertical shear of large-scale environmental flow. The data are available 4 times daily, and they have a horizontal resolution of 2.5° latitude–longitude with 17 vertical levels on the pressure surfaces.

The translational speed of a TC was calculated using the centered time differencing based on the observed changes in longitude and latitude at 6-h intervals, except for the first and last records in which a one-sided time differencing was used. The vertical shear is estimated from the NCEP–NCAR reanalysis, and it is defined as the difference of total winds between 200 and 850 hPa, averaged within a circle of 5° latitude around the TC center in this study. This is consistent with that used for the western North Pacific in ZWW. The upper-tropospheric outflow layer temperature T_{out} is calculated as the coldest upper-level temperature near the tropopause, averaged within a radius of 5° latitude around the TC center. As presented by Bister and Emanuel (1998), the theoretical MPI measured by the near-surface wind speed is proportional to the thermodynamic efficiency, which is defined as

$$\varepsilon = \sqrt{\frac{\mathrm{SST} - T_{\mathrm{out}}}{T_{\mathrm{out}}}}. \quad (1)$$

The thermodynamic efficiency is determined by both SST and outflow layer temperature, but it is highly correlated to SST (ZWW).

3. Thermodynamic control of TC MPI

a. An SST-determined empirical MPI

SST determines the amount of sensible and latent heat available to a TC from the ocean. Thus, it is indicative of the potential TC maximum intensity (Miller 1958; Malkus and Riehl 1960). We first explore the relationship between TC intensity and SST and construct an empirical TC MPI as a function of SST over the Atlantic Ocean. Following DeMaria and Kaplan (1994a), Whitney and Hobgood (1997), and ZWW, we also subtracted the translational speed from the maximum sustained surface wind speed (hereafter V_{max}) of the best track to eliminate the influence of storm motion on the estimated storm intensity. The resultant maximum sustained surface wind speed is defined as the intensity of the TC used for the rest of our analysis.

Figure 1a shows the scatter diagram of storm intensity against SST. Consistent with previous studies (DeMaria and Kaplan 1994a; Whitney and Hobgood 1997; ZWW), strong TCs occurred only over high SSTs, and a large number of weak TCs over the high SSTs represents the early stages of TC development in the tropics. This also explains why most intense TCs are not collocated with the warmest SST (because of the predominant poleward movement after their formation). A considerable number of TCs occurred over SSTs below 25°C, indicating that although TCs can only form over warm SST (Gray 1968), once they develop, they can survive over oceans with lower SSTs. These storms were generally weak, or they were experiencing an extratropical transition. Comparing Fig. 1a herein and Fig. 1a in ZWW, we can see higher (lower) maximum intensities over SSTs below (above) 25°C in the Atlantic Ocean than those in the western North Pacific, indicating the TC is often stronger (weaker) over SSTs below (above) 25°C in the Atlantic than those in the western North Pacific.

To quantify the relationship between TC intensity and SST, we stratified the observations to each 1°C SST group following DeMaria and Kaplan (1994a). Each group was assigned to the nearest midpoint SST.

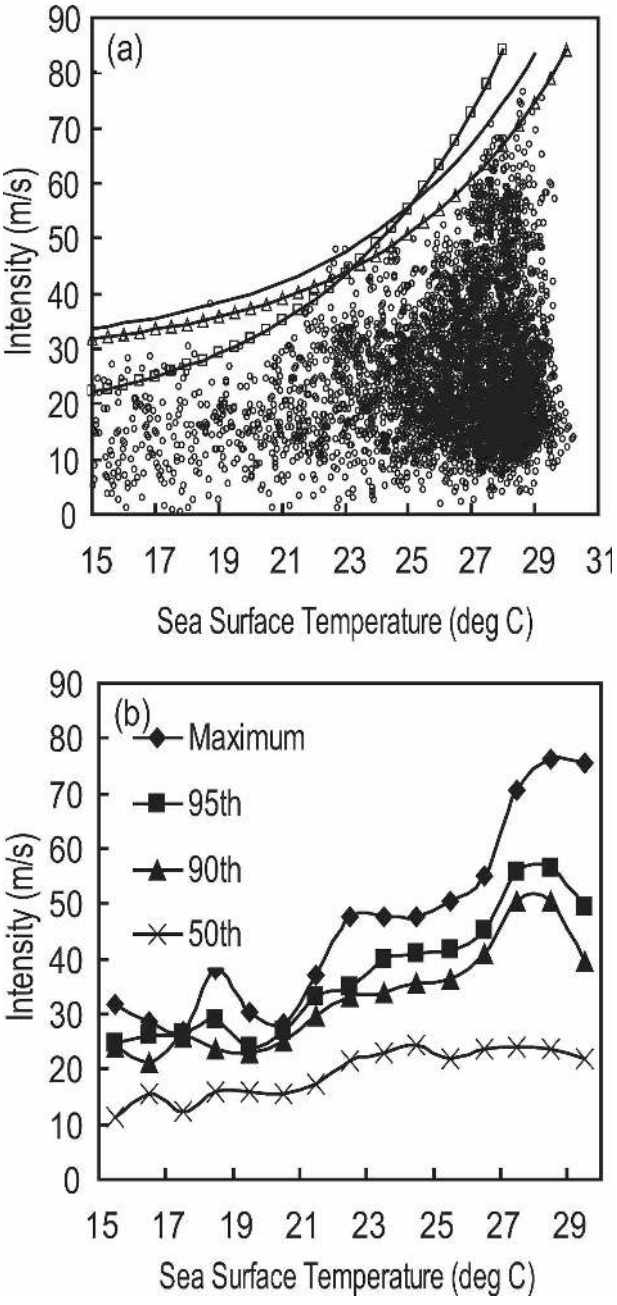

FIG. 1. (a) Scatter diagram of TC intensity (maximum surface sustained wind in m s^{-1}) vs SST (°C) over the Atlantic during 1981–2003. Intensity was corrected by subtracting storm translational speed: EMPI (m s^{-1}) as a function of SST (°C) derived for the Atlantic (solid curve); EMPI for the Atlantic (solid curve with triangle) from DeMaria and Kaplan (1994a); and EMPI for western North Pacific (solid curve with square) from Zeng et al. (2007). (b) Maximum intensity and 95th, 90th, and 50th intensity percentiles for each 1°C SST group as defined in DeMaria and Kaplan (1994a) vs SST.

TABLE 1. Properties of SST groups.

SST midpoint (°C)	No. of observations	Avg intensity (m s^{-1})	Avg top 50% intensity (m s^{-1})
15.5	39	13.34	19.46
16.5	36	15.09	20.51
17.5	43	14.06	20.58
18.5	40	15.42	20.63
19.5	50	15.98	20.35
20.5	68	16.19	21.53
21.5	91	19.17	25.62
22.5	133	21.84	29.78
23.5	185	23.51	31.09
24.5	304	24.10	31.80
25.5	433	23.83	31.50
26.5	719	25.40	34.45
27.5	1181	27.49	38.97
28.5	1198	27.68	38.99
29.5	272	24.96	33.53
30.5	5	14.11	14.97

Table 1 shows the features of all 16 groups of SSTs. About 70% of the observations (i.e., 3375 out of 4807) were assigned to SST categories greater than 26°C, about 12% lower than those found in the basin in 1962–92 by DeMaria and Kaplan (1994a). Note that the highest average intensity of total systems or top 50% intense systems occurred in the 28.5°C group. The maximum intensity, the 95th, 90th, and 50th intensity percentiles for each 1°C SST group, as shown in Fig. 1b, displays an increase in SST until a decrease at very high SSTs larger than 28.5°C, similar to the results of DeMaria and Kaplan (1994a) for the Atlantic and ZWW for the western North Pacific.

An EMPI as a function of SST, similar to that developed by DeMaria and Kaplan (1994a), can be constructed. Instead of using the climatological SST in DeMaria and Kaplan, we used the Reynolds weekly SST linearly interpolated in time and spatially interpolated to the TC center following the best track. The maximum intensity (surface sustained maximum wind speed corrected by subtracting translation speed) can be fitted to an exponential function of SST:

$$\mathrm{MPI} = A + Be^{C(\mathrm{SST}-T_0)}, \tag{2}$$

where $A = 29.5$ m s^{-1}, $B = 64.6$ m s^{-1}, $C = 0.1813$°C^{-1}, and $T_0 = 30.0$°C. The fitted curve is given in Fig. 1a. This exponential function is the same as that obtained by DeMaria and Kaplan (1994a). However, the fitted constants A and B are different [A and B are 28.2 and 55.8 m s^{-1}, respectively, in DeMaria and Kaplan (1994a)], but C is the same. The same slope parameter C in (2) in the two studies for two different periods indicates a stable trend of maximum TC intensity with

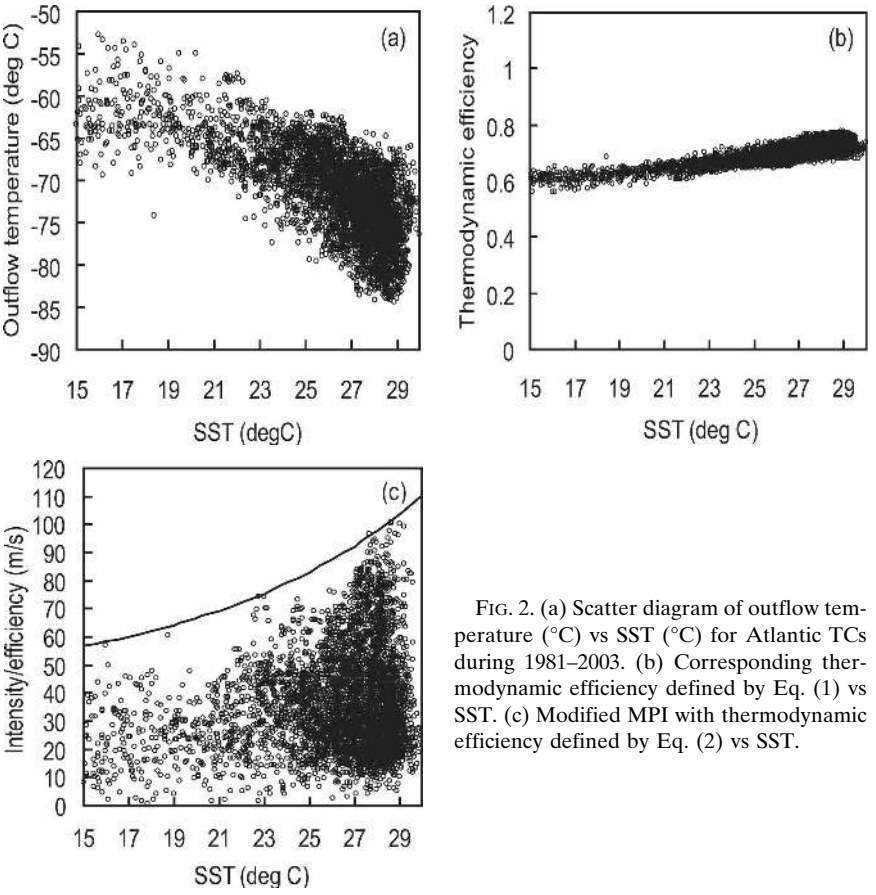

FIG. 2. (a) Scatter diagram of outflow temperature (°C) vs SST (°C) for Atlantic TCs during 1981–2003. (b) Corresponding thermodynamic efficiency defined by Eq. (1) vs SST. (c) Modified MPI with thermodynamic efficiency defined by Eq. (2) vs SST.

SST in the Atlantic. Because they used the climatological SST, which is usually smaller than the weekly SST, the fitted constants A and B are larger in our study than in theirs, indicating that for a given SST, the MPI could be slightly higher in the period we studied than that studied by DeMaria and Kaplan. This result implies that factors other than SST could be more favorable to TC intensity in the later period than in the earlier period. Note that the SST-determined EMPI not only includes the thermodynamic control of SST but also implicitly includes the dynamical effects from the environmental flow and vertical shear because the latter are not completely independent of SST in the basin.

b. An EMPI with thermodynamic efficiency

The difference between SST and upper-level outflow layer temperature stands for the tropospheric thermodynamic stability, which is directly related to the thermodynamic efficiency of the TC Carnot heat engine (Emanuel 1988, 1995). Figure 2a shows the scatter diagram of outflow layer temperature against SST. Overall, outflow layer temperature and SST are negatively correlated but with a relatively wide spread. However, the thermodynamic efficiency defined in Eq. (1) is approximately a linear function of SST (Fig. 2b). Therefore, the EMPI given in (2) can be considered implicitly, including both the effect of thermodynamic efficiency and the dynamical control.

The mean outflow layer temperatures (about −63°C) for SST below 19°C over the Atlanticare higher than those (about −68°C) of the western North Pacific (cf. Fig. 2a in ZWW), resulting in a slightly lower (about 0.6) mean thermodynamic efficiency (Fig. 2b) than that (slightly above 0.6) of the western North Pacific. One of the reasonable explanations for the higher outflow layer temperatures for SST below 19°C over the Atlantic is the tropospheric depth, which is generally lower in the North Atlantic than in the western North Pacific.

To verify the direct effect of dynamical control on TC MPI in the next section, we modify the original SST-determined EMPI given in (2) to explicitly include the effect of thermodynamic efficiency as follows:

$$\mathrm{MPI}^M = \varepsilon[A' + B' e^{C'(\mathrm{SST}-T_0)}], \tag{3}$$

where $A' = 41.5\ \mathrm{m\ s^{-1}}$, $B' = 68.6\ \mathrm{m\ s^{-1}}$, $C' = 0.1003°\mathrm{C}^{-1}$, and $T_0 = 30.0°\mathrm{C}$. Note that we use the

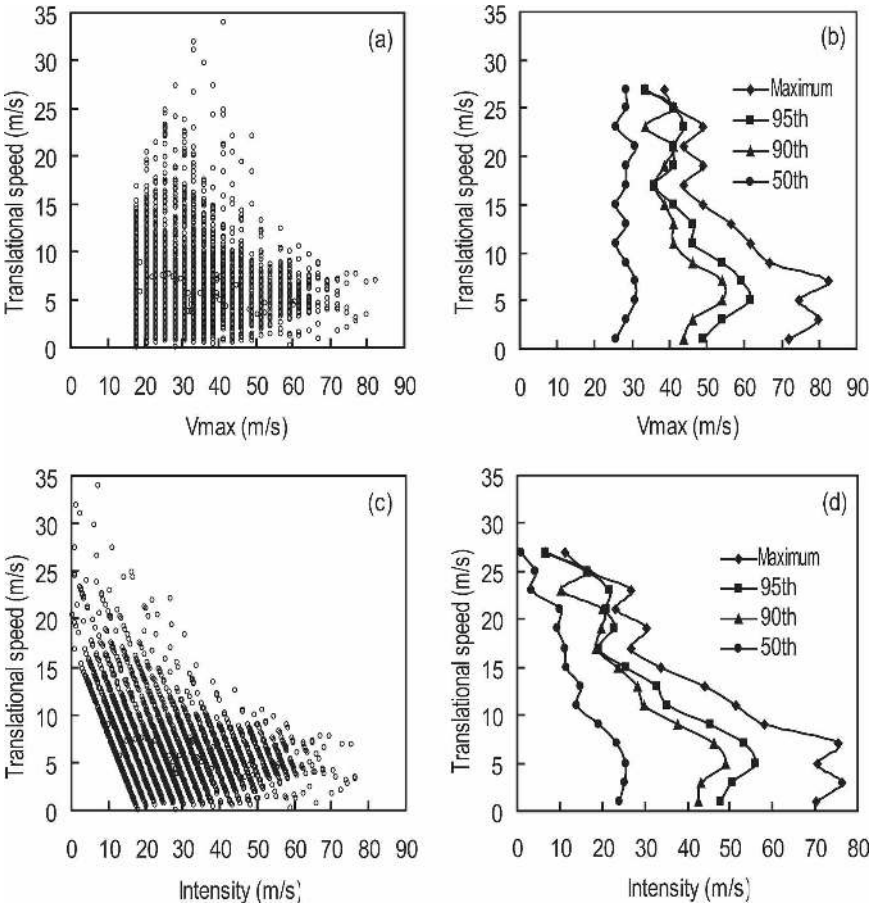

FIG. 3. Scatter diagrams of TC intensity ($m\ s^{-1}$) vs translational speed ($m\ s^{-1}$) from (a) best-track intensity and (c) corrected by subtracting storm translational speed for TCs over the Atlantic during 1981–2003. (b), (d) Corresponding maximum intensity and 95th, 90th, 50th intensity percentiles for each 2 $m\ s^{-1}$ translational speed group vs translational speed.

superscript *M* to represent the EMPI with the modification to include the effect of thermodynamic efficiency. As a result, Eq. (3) can be considered to include the thermodynamic control explicitly and the dynamical control implicitly. Figure 2c gives the curve for the modified EMPI divided by the thermodynamic efficiency as a function of SST, which shows a much smaller slope than that for the western North Pacific given in ZWW (see their Fig. 13a). This much smaller slope is mainly caused by the relatively higher intensity and slightly lower thermodynamic efficiencies at low SSTs in the Atlantic than those in the western North Pacific.

4. Dynamical control of TC intensity

The environmental dynamical control of TC intensity discussed in this study includes the translational speed and vertical shear of environmental horizontal wind. In this section, we will first discuss the individual effects of the translational speed and vertical shear on TC intensification and intensity then discuss their combined effect, and then finally construct a TC EMI that incorporates the environmental dynamical control.

a. Effect of translation on TC intensity

Figure 3a shows the scatter diagram of TC intensity V_{max} without the correction of storm translation against the storm translational speed for the Atlantic TCs during the period from 1981 to 2003. It displays an overall decreasing trend of upper-bound intensity with an increasing translational speed, a feature similar to that in the Australian region (Wang and Wu 2004) and the western North Pacific (ZWW). We can see that very intense TCs (with maximum surface sustained wind speed greater than 65 $m\ s^{-1}$) appear to develop under a narrow range of translational speeds (between 3 and 8 $m\ s^{-1}$). This indicates that either a too fast or a too slow

TABLE 2. Properties of translational speed groups. V_{max} is the translation-corrected intensity of a TC.

Translational speed midpoint ($m\ s^{-1}$)	No. of observations	Avg best-track intensity ($m\ s^{-1}$)	Avg top 50% best-track intensity ($m\ s^{-1}$)	Avg V_{max} ($m\ s^{-1}$)	Avg top 50% V_{max} ($m\ s^{-1}$)
1.00	382	28.73	36.12	27.32	34.79
3.00	1040	30.64	39.50	27.55	36.42
5.00	1339	33.28	43.82	28.27	38.85
7.00	933	33.23	43.62	26.31	36.76
9.00	545	30.66	39.23	21.79	30.44
11.00	238	27.70	34.82	16.84	23.95
13.00	121	28.57	36.05	15.58	23.09
15.00	98	28.03	34.02	13.15	19.07
17.00	43	28.83	32.62	12.04	15.93
19.00	22	30.40	36.25	11.42	17.36
21.00	17	31.78	36.59	11.01	16.06
23.00	16	30.06	34.40	7.41	11.88
25.00	6	33.44	40.30	8.97	15.81
27.00	3	33.44	36.01	6.30	9.00
29.00	1	36.01	36.01	6.21	6.21
31.00	2	33.44	33.44	1.96	2.38

translation seems to inhibit TCs from becoming too strong. As discussed in Wang and Wu (2004) and ZWW, this trend can be explained by previous theoretical and numerical studies about oceanic cooling (Schade and Emanuel 1999; Schade 2000) and asymmetric structure (Shapiro 1983; Peng et al. 1999; Emanuel 2000). Similar to that discussed for the western North Pacific (ZWW), the few cases with a rapid translation speed are mainly associated with storms that recurved into the strong midlatitude westerly and experienced extratropical transition. These general features remain unchanged, even after the translational speed was subtracted from the best-track intensity (Fig. 3c).

To quantify the general trends seen in Figs. 3a and 4c, we stratified the observations based on each 2 $m\ s^{-1}$ translational speed group (Table 2). Similar to the results shown in Table 1 for SST, each observation was assigned to the nearest midpoint translational speed group. About 88% of the observations (4239 out of 4807) were assigned to the groups with a translational speed slower than or equal to 10 $m\ s^{-1}$, whereas 93% of the observations have a translational speed slower than or equal to 10 $m\ s^{-1}$ in the western North Pacific (see Table 2 in ZWW). Similar to the western North Pacific, the highest average translation-corrected intensity of the total systems or the top 50% intense systems occurred in the 5 $m\ s^{-1}$ translational group. In general, the average (best track) intensity of total systems and average (best track) top 50% intensity in the Atlantic are a bit smaller than those in the western North Pacific (see Table 2 in ZWW). This is particularly true for translational speeds between 1 and 15 $m\ s^{-1}$, which is consistent with the TC MPI in the Atlantic being a bit smaller than that in the western North Pacific, where SSTs are greater than 25°C (Fig. 1a). Note that the results for a translational speed larger than 15 $m\ s^{-1}$ are not representative because there are too few samples.

Figures 3b and 3d show the corresponding maximum TC intensity and the 95th, 90th, and 50th intensity percentiles for each 2 $m\ s^{-1}$ translational speed group. Because our focus is mainly on the possible effect of translational speed on the maximum TC intensity, we are mostly interested in the top 90% intense TCs. Regardless of the subtraction of the translational speed, the top 90% intense TCs generally occur in a narrow range (3–8 $m\ s^{-1}$), and they decrease with both the increase and the decrease of the translational speed (Figs. 3b and 3d). In general, these features are very similar to those for the western North Pacific TCs given in ZWW.

To partially isolate the effect of translational speed on TC intensity from that of SST, as done in ZWW, we define the relative intensity as the percentage of the translation-corrected TC intensity (V_{max}) to the SST-determined MPI ($100\%V_{max}$/MPI) and the relative lifetime peak intensity as the percentage of the translation-corrected lifetime peak intensity (C_{max}) to the SST-determined MPI at the time of peak intensity ($100\%C_{max}$/MPI). The scatter diagrams of the relative intensity and relative lifetime peak intensity against translational speed are given in Figs. 4a and 4c, respectively. The corresponding maximum, the 95th, 90th, and 50th relative intensity and relative lifetime peak intensity percentiles for each 2 $m\ s^{-1}$ translational speed group are shown in Figs. 4b and 4d. Figure 4 shows an increasing trend of relative TC intensity with decreasing translational speed (Figs. 4a and 4b), similar to the results shown in Figs. 3a and 3b, indicating an overall negative effect of translational speed on TC intensity.

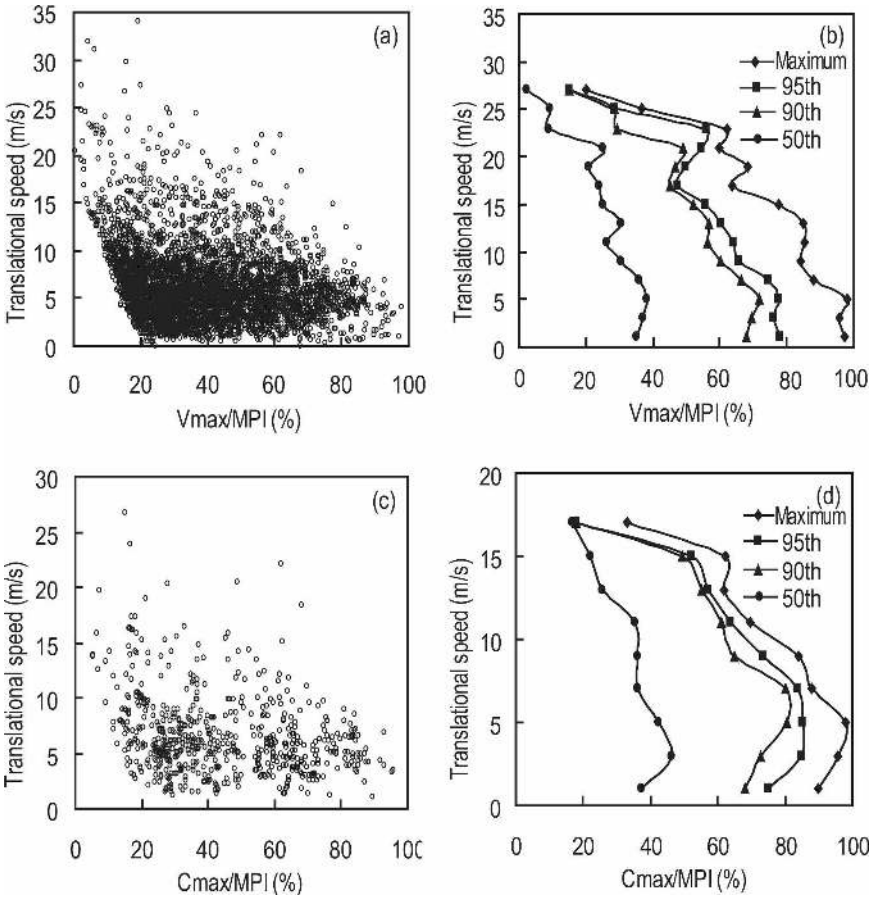

FIG. 4. Scatter diagram of (a) relative intensity (100%V_{max}/MPI) and (c) relative lifetime peak intensity (100%C_{max}/MPI) vs translational speed (m s^{-1}) over the Atlantic during 1981–2003; both V_{max} and C_{max} in m s^{-1} are corrected for storm translation. (b), (d) Corresponding maximum relative intensity and 95th, 90th, and 50th relative intensity percentiles for each 2 m s^{-1} translational speed group.

The relationship between the relative lifetime peak intensity and translational speed (Figs. 4c and 4d) has a similar feature to the relative intensity seen in Figs. 4a and 4b. Note that the relative lifetime peak intensity occurs at relatively low translational speeds, which is consistent with most TCs reaching their lifetime peak intensity just prior to recurvature, where the environmental steering flow is generally weak (Evans and McKinley 1998). The increasing trend of the relative intensity with the decreasing translational speed indicates that the fast translation is one of the limiting factors to TC intensity. This is consistent with the numerical results of Peng et al. (1999), who found that the surface friction and heat and moisture fluxes under a fast-translating storm could be quite asymmetric, thus inducing strong asymmetric structure, which is unfavorable to storm intensity.

Emanuel (2000) provided an alternative view on this effect based on energetic consideration. He proposed that the contribution by the asymmetric component to the volume-integrated entropy flux tends to be 0 because of its quasi-linear dependence on the total ground-relative wind. However, the asymmetric component in the ground-relative wind fields can have a net contribution to the volume-integrated surface frictional dissipation rate, which varies as the cube of the ground-relative wind speed. As a result, the net frictional dissipation rate resulting from the fast storm translation implies a weaker storm than that implied from the axisymmetric storm. This is indeed the case not only for the Atlantic TCs, but also for other ocean basins, such as the Australian region (Wang and Wu 2004) and the western North Pacific (ZWW).

b. Effect of vertical shear on TC intensity

Figure 5 shows the scatter diagrams of TC intensity, without and with translation correction, respectively, against the vertical shear and the corresponding maxi-

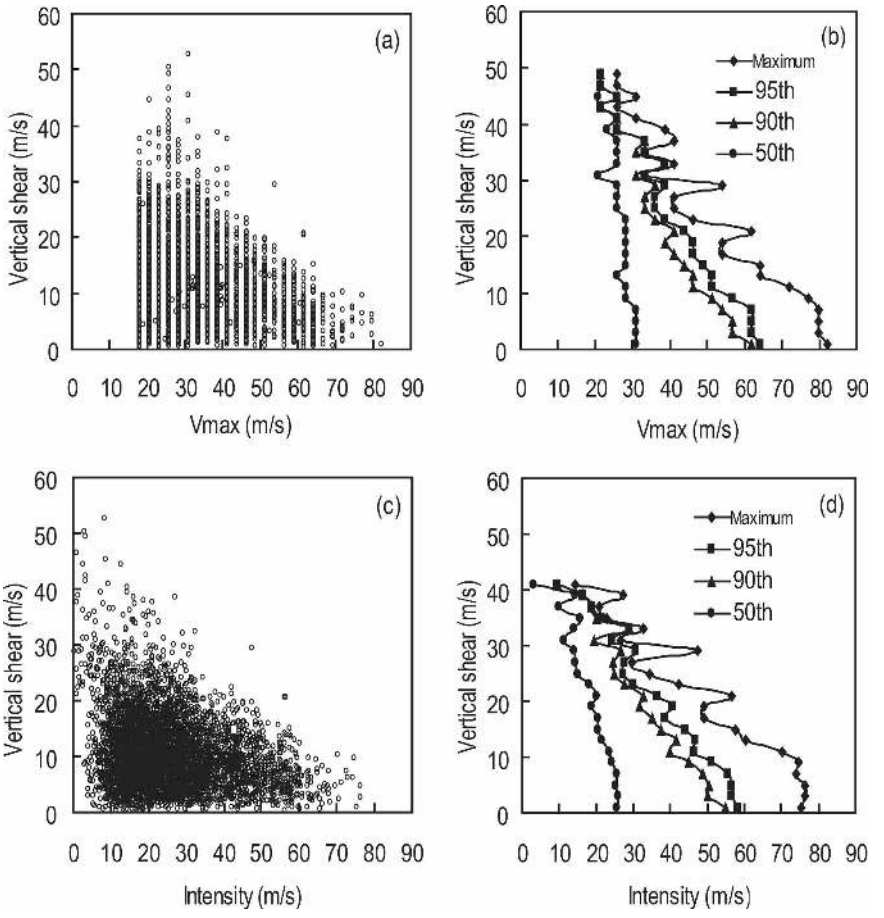

FIG. 5. Same as Fig. 3, but for vertical shear (m s^{-1}) and 2 m s^{-1} vertical shear group.

mum intensity, and the 95th, 90th, and 50th intensity percentiles for each 2 m s^{-1} vertical shear group. Table 3 lists the stratification and the general properties of the vertical shear groups for both the best-track intensity and the translation-corrected intensity. In general, there is an increasing trend of TC intensity with decreasing vertical shear. The average (best track) intensity of total systems or average (best track) top 50% intensity in the Atlantic is a bit smaller than those in the western North Pacific (see Table 2 in ZWW), which is consistent with the TC MPI in the Atlantic being a bit smaller than in the western North Pacific for SST higher than 20°C (Fig. 1). Although the vertical shear has an overall negative effect on TC intensity, very strong TCs can still survive in quite strong vertical shears, but very few intense TCs occur when the vertical shear is larger than 20 m s^{-1}, indicating that once TCs are strong enough, they could resist quite strong vertical shear, which is consistent with the simulation results of Wang et al. (2004) and the recent observational study of the western North Pacific by ZWW.

The scatter diagrams for both relative intensity and relative lifetime peak intensity against vertical shear are shown in Fig. 6. Similar to those shown in Fig. 5, there is a general increasing trend of the upper bounds of the relative intensity and relative lifetime peak intensity with decreasing vertical shear (Figs. 6a and 6c). The maximum, the 95th and 90th relative intensity and relative lifetime peak intensity percentiles for each 2 m s^{-1} vertical shear group (Figs. 6b and 6d), all decrease predominantly with increasing vertical shear, indicating an overall negative effect of vertical shear on TC intensity. Note that the decreasing slope of the relative lifetime peak intensity against vertical shear (Fig. 6c) is not as marked as that of the relative intensity (Fig. 6a). This appears to be because the possible delayed effect of vertical shear on TC intensity is not taken into account in our analysis.

c. Combined effect of translation and vertical shear

As we discussed above, both the vertical shear and translational speed have negative effects on TC intensity. Because the correlation coefficient between vertical shear and translational speed is only about 0.1023,

TABLE 3. Properties of the vertical shear groups.

Vertical shear midpoint ($m\,s^{-1}$)	No. of observations	Avg best-track intensity ($m\,s^{-1}$)	Avg top 50% best-track intensity ($m\,s^{-1}$)	Avg V_{max} ($m\,s^{-1}$)	Avg top 50% V_{max} ($m\,s^{-1}$)
1.00	144	35.02	47.69	29.71	42.82
3.00	442	33.60	44.90	28.24	40.04
5.00	610	33.71	44.80	28.20	39.51
7.00	660	33.20	43.79	27.76	38.74
9.00	666	32.15	41.89	26.66	36.69
11.00	569	30.59	39.13	24.96	33.71
13.00	488	30.48	38.91	24.60	33.12
15.00	381	29.51	37.33	23.25	31.25
17.00	248	29.09	36.14	22.25	29.38
19.00	195	28.57	35.25	21.06	28.13
21.00	120	29.90	36.70	21.19	28.65
23.00	82	27.60	33.50	18.16	25.09
25.00	69	25.66	30.94	15.63	21.87
27.00	41	27.29	32.21	15.36	21.65
29.00	32	27.17	33.60	15.61	23.54
31.00	14	23.70	28.66	12.31	18.18
33.00	7	28.29	33.44	19.34	24.58
35.00	13	27.11	29.76	14.10	19.21
37.00	9	27.15	31.38	11.51	16.38
39.00	6	26.15	30.01	13.79	19.88
41.00	3	27.44	28.30	9.04	11.95
43.00	1	25.72	25.72	3.40	3.40
45.00	3	25.72	28.30	8.12	10.81

their combined effect can be simply measured by a linear combination. Following ZWW, we introduce an equivalent dynamical speed U_{ST}, the combined magnitude of vertical shear (V_{shear}) and translation speed (V_{trans}):

$$U_{ST} = \sqrt{0.6V_{shear}^2 + (V_{trans} - 5)^2}. \quad (4)$$

As indicated in ZWW, a constant 5 $m\,s^{-1}$ is subtracted from the translational speed to take into account the negative effect of ocean mixing for slow-moving TCs (also see Fig. 3). Although (4) was tuned for the western North Pacific in ZWW, we found that it is also a good measure of the combined effect of vertical shear and translational speed on TCs in the Atlantic basin.

Figure 7 shows the scatter diagrams of TC intensity (Fig. 7a) and lifetime peak intensity (Fig. 7c) against U_{ST} and also shows the corresponding maximum intensity and the 95th, 90th, and 50th intensity percentiles for each 3 $m\,s^{-1}$ U_{ST} group (Figs. 7b and 7d), respectively. The upper bounds of both the intensity and lifetime peak intensity increase with decreasing U_{ST}, which is consistent with the individual effects from translational speed and vertical shear. The stratification and the general properties of the U_{ST} groups for TC intensity (V_{max}) and lifetime peak intensity (C_{max}) are given in Tables 4 and 5, respectively. We can see that both the average (lifetime peak) intensity and the average top 50% (lifetime peak) intensity, and the top intensity percentiles of both the intensity and lifetime peak intensity for each U_{ST} group increase as the combined magnitude U_{ST} of vertical shear and translation decreases, which is consistent with the individual effects from translational speed (Fig. 3) and vertical shear (Fig. 5), respectively. Similar characteristics can be found for the relative intensity ($100\%V_{max}$/MPI) and relative lifetime peak intensity ($100\%C_{max}$/MPI) as shown in Fig. 8. These results indicate that it is possible to add one more dimension to the upper limit of possible TC maximum intensity, namely the empirical MPI, by introducing the combined effect of vertical shear and translational speed.

d. An EMI incorporating environmental dynamical control

Following ZWW, we introduce the dynamical efficiency η defined as

$$\eta = 1/[1 + (U_{ST}/U_0)], \quad (5)$$

where U_0 is taken to be 60 $m\,s^{-1}$ and used to normalize the combined measure of the magnitude of vertical shear and translation parameter. The dynamical efficiency represents a nondimensional attenuation factor resulting from the combined negative effect of transla-

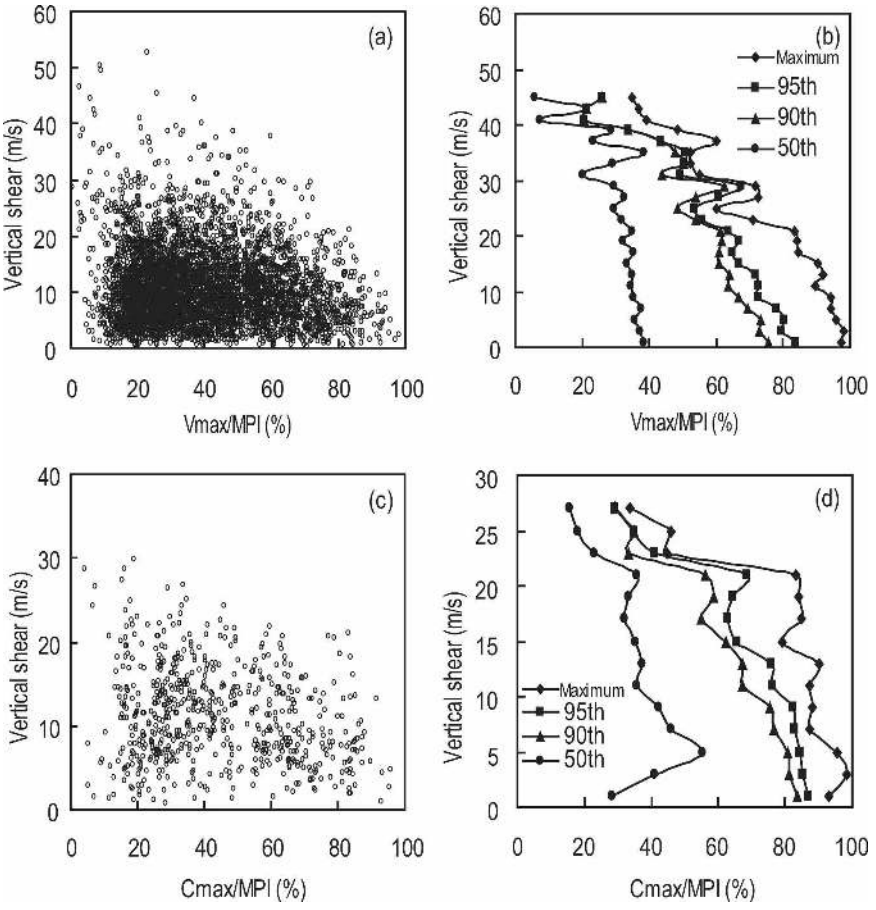

FIG. 6. (a), (c) Same as Fig. 4, but vs vertical wind shear ($m\ s^{-1}$). (b), (d) Corresponding maximum relative intensity and 95th, 90th, and 50th relative intensity percentiles for each 2 $m\ s^{-1}$ vertical shear group.

tion and vertical shear, in a very similar manner to the thermodynamic efficiency. Combining thermodynamic effect with dynamical control, we can obtain an EMI for Atlantic TCs as

$$\mathrm{EMI} = \eta \mathrm{MPI}^M = \eta\varepsilon[A' + B' e^{C'(\mathrm{SST}-T_0)}]. \qquad (6)$$

As we can see from Eq. (6), the dynamical control of TC intensity appears in the EMI in a transparent way. The MPI modified with the thermodynamic efficiency is reduced by a factor of the dynamical efficiency. To distinguish this dynamically modified EMI from the empirically determined MPI^M, we simply call this new maximum intensity the EMI. Different from the original SST-determined EMPI given in Eq. (2) and the modified EMPI, including the effect of thermodynamic efficiency in Eq. (3), which implicitly includes dynamical control, the new EMI (6) explicitly includes both the positive effect of SST and the negative effects of translation and vertical shear.

The dynamical efficiency (5) is inversely proportional to the magnitude of the combined vertical shear and translational speed. This gives a physically consistent asymptotic limit of the EMI, that is, as the vertical shear or translational speed or their combination becomes very large or infinite, the EMI approaches 0. On the other hand, when the dynamical efficiency becomes 1.0, that is, without the negative effect from the environmental dynamical control, the EMI approaches the thermodynamically determined MPI. Therefore, the SST-determined EMPI or that modified with the thermodynamic efficiency, only provides an upper limit of the maximum intensity regardless of the vertical shear or translational speed.

Note that the EMI (6) gives not only a measure of the dynamical control on TC maximum intensity but also gives a more accurate estimation of TC maximum intensity because it includes extra information about the limiting factors resulting from translational speed and vertical shear. Because the dynamical efficiency η (5) is positive and always smaller than unity, the EMI (6) is

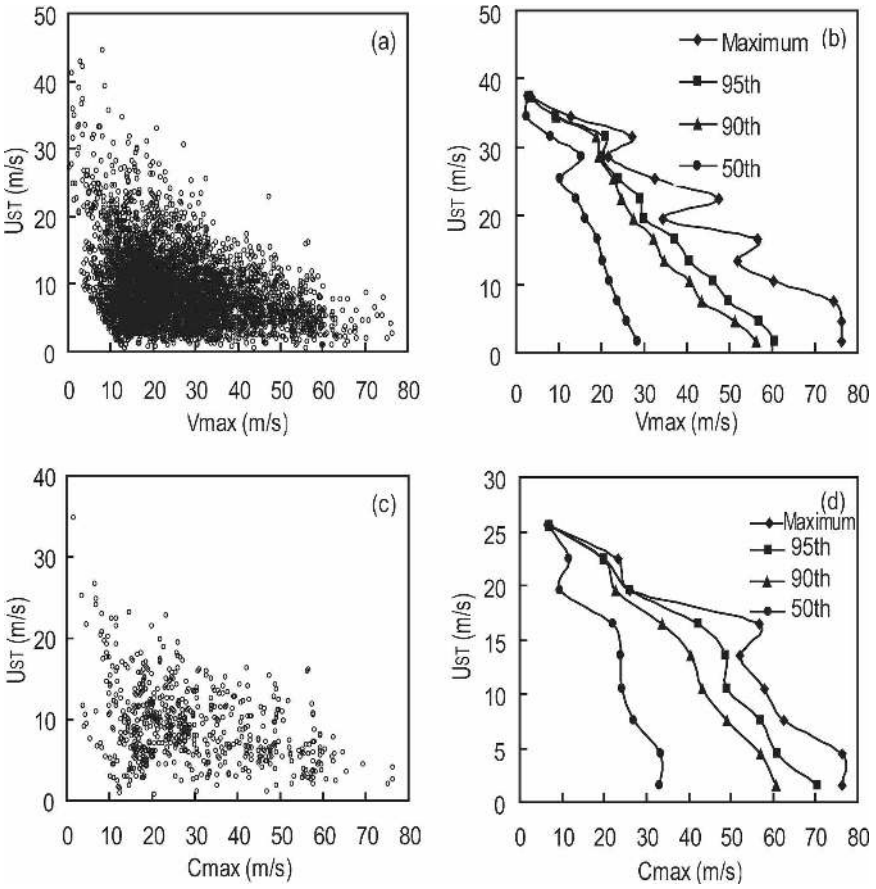

FIG. 7. Scatter diagrams of (a) intensity (V_{max}) and (c) lifetime peak intensity (C_{max}) against combined effect of storm translation and environmental vertical shear (m s^{-1}) over the Atlantic during 1981–2003. (b), (d) Corresponding 95th, 90th, and 50th intensity percentiles for each 3 m s^{-1} combined vertical shear and translational speed group.

TABLE 4. Properties of U_{ST} groups for translation-corrected and relative intensity.

U_{ST} midpoint (m s^{-1})	No. of observations	Avg V_{max} (m s^{-1})	Avg top 50% V_{max} (m s^{-1})	Avg V_{max}/MPI (%)	Avg top 50% V_{max}/MPI (%)
1.50	320	31.24	43.80	44.09	61.83
4.50	1181	28.77	40.18	41.43	58.39
7.50	1296	26.11	35.81	38.73	53.92
10.50	954	24.27	32.83	38.09	52.29
13.50	496	22.08	29.41	37.26	51.19
16.50	256	20.66	27.61	37.00	50.09
19.50	143	17.15	23.51	33.26	45.81
22.50	74	15.28	21.73	33.23	47.58
25.50	38	12.03	18.29	27.22	40.55
28.50	20	12.66	17.59	30.00	42.98
31.50	12	11.17	17.74	25.13	39.27
34.50	9	5.44	8.24	14.24	21.42
37.50	3	3.12	3.31	6.59	6.97
40.50	3	4.40	6.10	12.37	17.36
43.50	2	5.61	8.21	15.62	22.72

TABLE 5. Properties of U_{ST} groups for translation-corrected lifetime and relative peak intensities.

U_{ST} midpoint ($m\ s^{-1}$)	No. of observations	Avg C_{max} ($m\ s^{-1}$)	Avg top 50% C_{max} ($m\ s^{-1}$)	Avg C_{max}/MPI (%)	Avg top 50% C_{max}/MPI (%)
1.50	38	37.25	55.98	51.95	77.16
4.50	125	35.48	49.85	51.77	72.68
7.50	167	29.91	40.97	44.87	62.94
10.50	148	26.56	35.41	41.54	56.27
13.50	81	25.62	33.72	41.80	56.13
16.50	49	23.70	31.54	40.89	55.10
19.50	14	14.72	20.38	27.17	35.99
22.50	8	13.13	17.43	24.88	34.94
25.50	4	6.07	7.00	13.85	16.47

always smaller than the thermodynamically determined MPI (3), which includes the effect of thermodynamic efficiency. This is consistent with the negative effects of translation and vertical shear on TC intensity.

Figure 9 compares the cumulative percentages of TCs reaching their SST-determined MPI, the modified MPI^M with thermodynamic efficiency, and the newly introduced EMI discussed in this study and given in (2), (3), and (6), respectively. We can see that the percentage of TCs reaching the EMI is considerably higher than that reaching either the MPI or MPI^M without explicitly including the dynamical efficiency, a feature that is the same as that found in ZWW (see their Fig. 14). However, as shown in Fig. 9 and Table 6, 48.72%

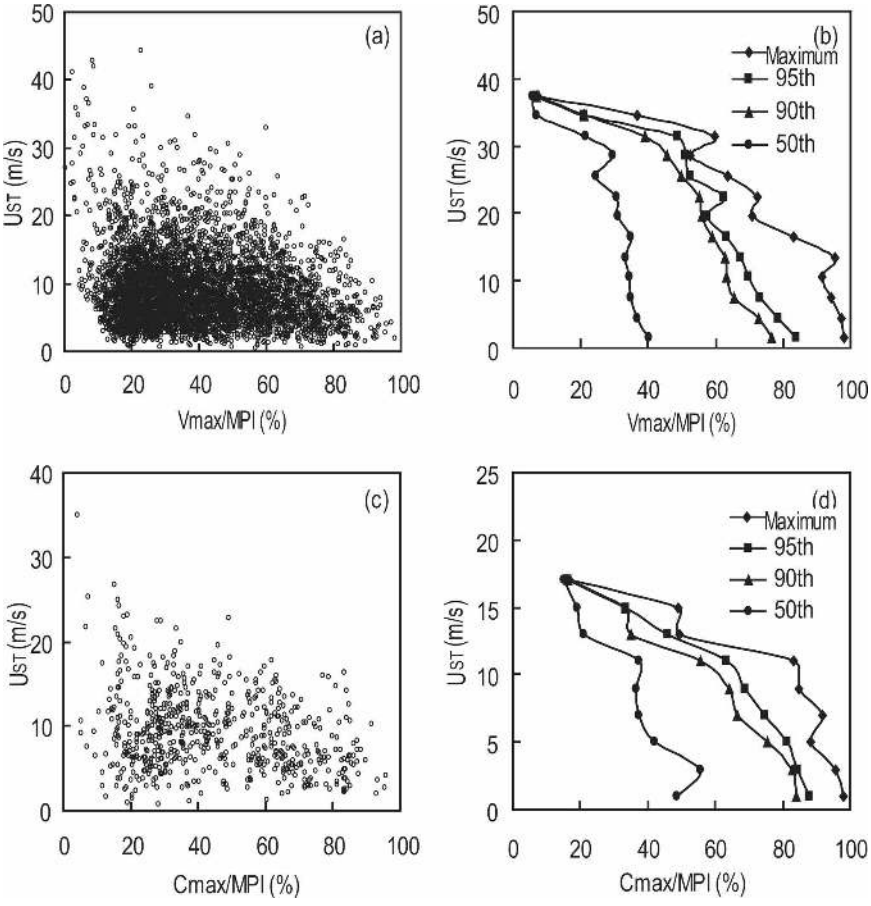

FIG. 8. Same as Fig. 7, but for relative intensity (100%V_{max}/MPI) and relative lifetime peak intensity (100%C_{max}/MPI).

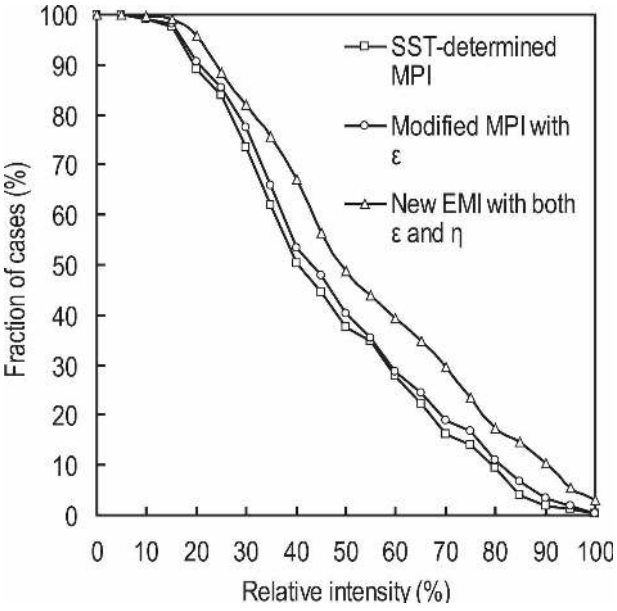

FIG. 9. Cumulative distributions of relative peak intensity from original SST-determined MPI (curve with squares), modified MPI with thermodynamic efficiency included (curve with circles), and new EMI incorporating environmental dynamical control (curve with triangles) for the Atlantic TCs during 1981–2003.

(17.52%) of the storms reached 50% (80%) of their EMI over the Atlantic. The cumulative percentage for TCs reaching 50% (80%) of their EMI is increased by 11.11% (8.12%) because of the explicit inclusion of both the dynamical and thermodynamic efficiencies, whereas a 5.87% (5.69%) increase was found in the western North Pacific (see Table 6 in ZWW). DeMaria and Kaplan (1994a) showed that about 20% of Atlantic TCs reach 80% or more of their MPIs at the time when they are most intense, whereas about 9.4% reach 80% or more of their original SST-determined MPI in this study. This implies that the percentage of most intense TC is decreasing because the MPI is higher for the period of 1981–2003 than for period they studied (see Fig. 1a).

5. Summary and discussion

In this study, based on the best-track TC data, Reynolds SST, and NCEP–NCAR reanalysis during 1981–2003, we have analyzed both the thermodynamic and dynamical controls of TC maximum intensity in the Atlantic. We show that both the vertical shear and translational speed have negative effects on TC intensity, which is consistent with that found for both the Australian region (Wang and Wu 2004) and western North Pacific (Zeng et al. 2007). The average (best track) intensity of total systems or average (best track) top 50% intensity in the Atlantic is a bit smaller than those in the western North Pacific. A robust result is that few TCs intensified when they moved with translational speeds larger than 15 m s^{-1}, which is similar to the value found for the western North Pacific. The threshold vertical shear of 20 m s^{-1} is found above which few TCs intensified and below which most TCs could reach their lifetime peak intensity. Very strong TCs can survive in relatively strong vertical shears over the Atlantic, which is in support of the numerical results of Wang et al. (2004) and the observations of the western North Pacific (Zeng et al. 2007).

We found an increase in the empirical MPI as a function of SST derived for Atlantic TCs during 1981–2003, compared with the similar MPI found in DeMaria and Kaplan (1994a) for the period of 1962–92. We also show that the mean outflow layer temperatures at SSTs below 19°C in the Atlantic are warmer than those in the western North Pacific. This gives a slightly lower mean thermodynamic efficiency for Atlantic TCs.

With the introduction of the dynamical efficiency, a new empirical maximum intensity (EMI) has been constructed, which includes the positive contribution by SST and the combined negative effect of translational speed and vertical shear as the environmental dynamical control of TC intensity. The new EMI provides a more accurate estimation of real TC maximum intensity and an approximate, explicit measure of the environmental dynamical control of TC maximum intensity. As a result, the newly developed EMI can be used operationally to improve the estimation of TC maximum intensity and to help improve our understanding of factors controlling TC intensity in the Atlantic.

Note that the SST-determined EMPI could differ considerably for the different ocean basins, such as the western North Pacific and North Atlantic (ZWW; DeMaria and Kaplan 1994a). It is likely due to the best-track intensity datasets, which have recently been documented by Kossin et al. (2007) and Knaff and Zehr (2007). Therefore, for practical use, specific EMPI should be developed for each basin. Nevertheless, regardless of the basins, the inclusion of dynamical control could improve the estimate of TC maximum intensity because it provides a higher percentage of storms reaching their newly developed EMI than those reaching their SST-determined MPI and the MPI modified to include the effect of the thermodynamic efficiency.

Most importantly, the dynamical efficiency that we have introduced does not appear to be basin dependent. It represents the negative effect of environmental dynamical control of TC maximum intensity. Therefore, our findings could be potentially generalized and

TABLE 6. Cumulative number of observations and cumulative percentage with relative intensity.

Relative intensity (%)	Original SST-determined MPI		MPI with thermodynamic efficiency		EMI with thermodynamic and dynamical efficiencies	
	Cumulative No. of observations	Cumulative percentage (%)	Cumulative No. of observations	Cumulative percentage (%)	Cumulative No. of observations	Cumulative percentage (%)
0	234	100.00	234	100.00	234	100.00
5	234	100.00	234	100.00	234	100.00
10	232	99.15	232	99.15	233	99.57
15	228	97.44	230	98.29	232	99.15
20	208	88.89	212	90.60	224	95.73
25	196	83.76	200	85.47	207	88.46
30	172	73.50	181	77.35	192	82.05
35	145	61.97	154	65.81	177	75.64
40	118	50.43	125	53.42	157	67.09
45	104	44.44	112	47.86	132	56.41
50	88	37.61	94	40.17	114	48.72
55	81	34.62	83	35.47	103	44.02
60	65	27.78	67	28.63	92	39.32
65	52	22.22	57	24.36	81	34.62
70	38	16.24	44	18.80	69	29.49
75	33	14.10	39	16.67	55	23.50
80	22	9.40	26	11.11	41	17.52
85	9	3.85	16	6.84	34	14.53
90	4	1.71	8	3.42	24	10.26
95	3	1.28	4	1.71	13	5.56
100	1	0.43	1	0.43	7	2.99

applied to other ocean basins. Finally, it should be mentioned that Atlantic TCs are often sheared between the low and midlevels, especially when systems are located in the tropical eastern Atlantic. This is due to the low-level African easterly jet. Though it might be inferred by the fast translational speed, this is not accounted for in the EMI formula because only deep-layer shear is calculated in this study. The effect of vertical profile of vertical shear on TC intensity is not yet well understood, and it is beyond the scope of this study; however, it will be a topic for our future studies.

Acknowledgments. The authors are grateful to three anonymous reviewers for their constructive comments, which helped improve the representation and quality of this work. This study has been supported by the NSF under Grant ATM-0427128, the U.S. Office of Naval Research under Grant N0014-06-10303, the National Natural Science Foundation of China under Grants 40575030 and 40730948, and the Typhoon Research Foundation of Shanghai Typhoon Institute/China Meteorological Administration under Grant 2006STB07.

REFERENCES

Bender, M. A., 1997: The effect of relative flow on the asymmetric structure in the interior of hurricanes. *J. Atmos. Sci.,* **54,** 703–724.

Bister, M., and K. A. Emanuel, 1998: Dissipative heating and hurricane intensity. *Meteor. Atmos. Phys.,* **50,** 233–240.

Chen, S. S., J. A. Knaff, and F. D. Marks Jr., 2006: Effects of vertical wind shear and storm motion on tropical cyclone rainfall asymmetries deduced from TRMM. *Mon. Wea. Rev.,* **134,** 3190–3208.

Corbosiero, K. L., and J. Molinari, 2002: The effects of vertical wind shear on the distribution of convection in tropical cyclones. *Mon. Wea. Rev.,* **130,** 2110–2123.

——, and ——, 2003: The relationship between storm motion, vertical wind shear, and convective asymmetries in tropical cyclones. *J. Atmos. Sci.,* **60,** 366–460.

DeMaria, M., 1996: The effect of vertical shear on tropical cyclone intensity change. *J. Atmos. Sci.,* **53,** 2076–2087.

——, and J. Kaplan, 1994a: Sea surface temperature and the maximum intensity of Atlantic tropical cyclones. *J. Climate,* **7,** 1325–1334.

——, and ——, 1994b: A statistical hurricane intensity prediction scheme (SHIPS) for the Atlantic basin. *Wea. Forecasting,* **9,** 209–220.

——, and ——, 1999: An updated statistical hurricane intensity prediction scheme (SHIPS) for the Atlantic and North Pacific basins. *Wea. Forecasting,* **14,** 326–337.

——, M. Mainelli, L. K. Shay, J. A. Knaff, and J. Kaplan, 2005: Further improvements to the statistical hurricane intensity prediction scheme (SHIPS). *Wea. Forecasting,* **20,** 531–543.

Elsberry, R. L., and R. Jeffries, 1996: Vertical wind shear influences on tropical cyclone formation and intensification during TCM-92 and TCM-93. *Mon. Wea. Rev.,* **124,** 1374–1387.

Emanuel, K. A., 1988: The maximum intensity of hurricanes. *J. Atmos. Sci.,* **45,** 1143–1155.

——, 1995: Sensitivity of tropical cyclones to surface exchange

coefficients and a revised steady-state model incorporating eye dynamics. *J. Atmos. Sci.,* **52,** 3969–3976.

——, 2000: A statistical analysis of hurricane intensity. *Mon. Wea. Rev.,* **128,** 1139–1152.

Evans, J. L., and K. McKinley, 1998: Relative timing of tropical storm lifetime maximum intensity and track recurvature. *Meteor. Atmos. Phys.,* **65,** 241–245.

Frank, W. M., and E. A. Ritchie, 1999: Effects of environmental flow upon tropical cyclone structure. *Mon. Wea. Rev.,* **127,** 2044–2061.

——, and ——, 2001: Effects of vertical wind shear on the intensity and structure of numerically simulated hurricanes. *Mon. Wea. Rev.,* **129,** 2249–2269.

Gray, M. W., 1968: Global view of the origin of tropical disturbances and storms. *Mon. Wea. Rev.,* **96,** 669–700.

Jones, S. C., 1995: The evolution of vortices in vertical shear. I: Initially barotropic vortices. *Quart. J. Roy. Meteor. Soc.,* **121,** 821–851.

Kalnay, E., and Coauthors, 1996: The NCEP/NCAR 40-Year Reanalysis Project. *Bull. Amer. Meteor. Soc.,* **77,** 437–471.

Knaff, J. A., and R. M. Zehr, 2007: Reexamination of tropical cyclone pressure wind relationships. *Wea. Forecasting,* **22,** 71–88.

——, C. R. Sampson, and M. DeMaria, 2005: An operational statistical typhoon intensity prediction scheme for the western North Pacific. *Wea. Forecasting,* **20,** 688–699.

Kossin, J. P., J. A. Knaff, H. I. Berger, D. C. Herndon, T. A. Cram, C. S. Velden, R. J. Murnane, and J. D. Hawkins, 2007: Estimating hurricane wind structure in the absence of aircraft reconnaissance. *Wea. Forecasting,* **22,** 89–101.

Lonfat, M., F. D. Marks Jr., and S. S. Chen, 2004: Precipitation distribution in tropical cyclones using the tropical rainfall measuring mission (TRMM) microwave imager: A global perspective. *Mon. Wea. Rev.,* **132,** 1645–1660.

Malkus, J. S., and H. Riehl, 1960: On the dynamics and energy transformation in steady-state hurricanes. *Tellus,* **12,** 1–20.

Merrill, R. T., 1988: Environmental influences on hurricane intensification. *J. Atmos. Sci.,* **45,** 1678–1687.

Miller, B. I., 1958: On the maximum intensity of hurricanes. *J. Meteor.,* **15,** 184–195.

NHC–TPC, cited 2006, Tropical cyclone best track data site. [Available online at http://weather.unisys.com/hurricane/atlantic/index.html.]

Peng, M. S., B.-F. Jeng, and R. T. Williams, 1999: A numerical study on tropical cyclone intensification. Part I: Beta effect and mean flow effect. *J. Atmos. Sci.,* **56,** 1404–1423.

Reasor, P. D., M. T. Montgomery, and L. D. Grasso, 2004: A new look at the problem of tropical cyclones in vertical shear flow: Vortex resiliency. *J. Atmos. Sci.,* **61,** 3–22.

Reynolds, R. W., N. A. Rayner, T. M. Smith, D. C. Stokes, and W. Wang, 2002: An improved in situ and satellite SST analysis for climate. *J. Climate,* **15,** 1609–1625.

Schade, L. R., 2000: Tropical cyclone intensity and sea surface temperature. *J. Atmos. Sci.,* **57,** 3122–3130.

——, and K. A. Emanuel, 1999: The ocean's effect on the intensity of tropical cyclones: Results from a simple coupled atmosphere–ocean model. *J. Atmos. Sci.,* **56,** 642–651.

Shapiro, L. J., 1983: The asymmetric boundary layer flow under a translation hurricane. *J. Atmos. Sci.,* **40,** 1984–1998.

Wang, Y., and G. J. Holland, 1996: Tropical cyclone motion and evolution in vertical shear. *J. Atmos. Sci.,* **53,** 3313–3332.

——, and C.-C. Wu, 2004: Current understanding of tropical cyclone structure and intensity changes—A review. *Meteor. Atmos. Phys.,* **87,** 257–278.

——, M. T. Montgomery, and B. Wang, 2004: How much vertical shear can a tropical cyclone resist? *Bull. Amer. Meteor. Soc.,* **85,** 661–662.

Whitney, L. D., and J. S. Hobgood, 1997: The relationship between sea surface temperatures and maximum intensities of tropical cyclones in the eastern North Pacific Ocean. *J. Climate,* **10,** 2921–2930.

Zeng, Z., Y. Wang, and C.-C. Wu, 2007: Environmental dynamical control of tropical cyclone intensity—An observational study. *Mon. Wea. Rev.,* **135,** 38–59.